Mapping Polymer Heterogeneity Using Atomic Force Microscopy Phase Imaging and Nanoscale Indentation

by

D. Raghavan and X. Gu
Howard University
Washington, DC, 20059, USA
and
T. Nguyen, M. VanLandingham and A. Karim
National Institute of Standards and Technology
Gaithersburg, MD 20899-8621 USA

Reprinted from the Macromolecules, Vol. 33, No. 7, 2573-2583, 2000.

Mapping Polymer Heterogeneity Using Atomic Force Microscopy Phase Imaging and Nanoscale Indentation

D. Raghavan,*,† X. Gu,† T. Nguyen,‡ M. VanLandingham,‡ and A. Karim§

Polymer Science Division, Department of Chemistry, Howard University, Washington, D.C. 20059; and Building and Fire Research Laboratory, Building Materials Division, and Materials Science and Engineering Laboratory, Polymer Division, National Institute of Standards and Technology, Gaithersburg, Maryland 20899

Received July 22, 1999; Revised Manuscript Received November 11, 1999

ABSTRACT: Polymer coatings often contain degradation-susceptible regions, and corrosion of the metallic substrate can occur directly underneath these regions. In this paper, the microstructure of model coating materials is investigated using atomic force microscopy (AFM). Specifically, AFM is used to study heterogeneity in thin film blends of polystyrene (PS) and polybutadiene (PB) as a function of annealing time at 80 °C. PS/PB blend films with thicknesses of approximately 250 nm are prepared by spin casting from solutions onto silicon substrates. Both topographic and phase imaging in tapping mode AFM are performed on these films under ambient conditions and at different force levels using a silicon tip. For certain force levels, phase imaging provides good contrast between the phase-separated PS and PB regions, primarily because of the large compliance difference between the two materials. This contrast decreases with increasing annealing time because thermal oxidation causes cross-linking in PB, and thus, the compliance of the PB region increases toward that of PS. Nanoscale indentation measurements are then made on the observed phase-separated regions to identify these regions as PS- and PB-rich and to better understand the influence of relative surface stiffness on the phase images. Cast and free-standing films of pure PS and pure PB are also studied as a function of annealing time using AFM, contact angle measurements, Fourier transform infrared spectroscopy (FTIR), differential scanning calorimetry (DSC), and dynamic mechanical analysis (DMA). Results from studies of the individual PS and PB films are related to the AFM results for the blend films. The use of phase imaging for cure monitoring of polymers and for studies of chemically heterogeneous polymer systems is also discussed.

Introduction

Major economic incentives exist for addressing the long-term performance of polymer coatings. For example, the United States Air Force (USAF) is faced with a major challenge to address the economics of air craft painting, stripping, repainting, and hazardous waste handling that currently exceeds $150 M per year.[1] In addition, corrosion-related problems are estimated to cost the USAF approximately $700 M per year. If the durability of these materials is to be enhanced, further research is needed to understand the structure of the coatings, investigate the changes that occur to the coatings upon exposure to aggressive environments, and relate these changes to the protective performance of the coatings.[2−3]

Polymer coatings can often be highly heterogeneous.[4−7] In recent years, extensive research has been conducted to characterize the heterogeneity in coatings, but these studies have been limited to indirect measurements such as microhardness, dc resistance, and ac impedance.[6,8,9] Polymer coatings can contain degradation-susceptible regions, and corrosion of metallic substrates has been found to occur directly underneath these regions.[4−12] The sizes of these regions are believed to range from nano- to micrometers. Micro- and spectroscopic techniques including electron microscopy, neutron and X-ray scattering, X-ray photoelectron spectroscopy, secondary-ion mass spectrometry, near-field scanning optical microscopy, and reflection optical microscopy have been used either in combination or independently to provide information about the morphology and composition of multicomponent polymer systems.[13−18] However, these techniques lack the lateral resolution needed to detect heterogeneity in polymer coatings. In addition, these techniques require a specific sample preparation procedure so that the sample is amenable for assay with the technique.

One technique that can provide direct spatial mapping of surface topography and surface heterogeneity with nanometer resolution is atomic force microscopy (AFM).[18−25] In AFM, a probe consisting of a sharp tip (nominal tip radius on the order of 10 nm) located near the end of a cantilever beam is scanned across the sample surface using piezoelectric scanners. Changes in the tip−sample interaction are often monitored using an optical lever detection system, in which a laser is reflected off of the cantilever and onto a position-sensitive photodiode. During scanning, a particular operating parameter is maintained at a constant level, and images are generated through a feedback loop between the optical detection system and the piezoelectric scanners.

Three imaging modes can be used to produce topographic images of sample surfaces, contact mode, noncontact mode, and tapping mode AFM (TMAFM). TMAFM tends to be more applicable to general imaging of soft samples, such as biological and polymeric materials, under ambient conditions[19−27] and was used exclusively in the work described in this paper. In tapping mode, the cantilever oscillates close to its first bending mode

* To whom the correspondence should be addressed. E-mail: draghavan@howard.edu.
† Howard University.
‡ Building Materials Division, NIST.
§ Polymer Division, NIST.

10.1021/ma991206r CCC: $19.00
Published on Web 03/17/2000

resonance frequency (normally on the order of 100 kHz) so that the tip makes contact with the sample only for a short duration in each oscillation cycle. As the tip approaches the sample, the tip−sample interactions alter the amplitude, resonance frequency, and phase angle of the oscillating cantilever. During scanning, the amplitude at the operating frequency is maintained at a constant level, called the set-point amplitude, by adjusting the relative position of the tip with respect to the sample. This method of operation results in lower surface forces, particularly lateral forces, compared to those of contact mode so less surface damage is inflicted while maintaining higher lateral resolution than can often be achieved with noncontact mode.[24]

One recent development in TMAFM is the use of the changes in phase angle of the cantilever probe to produce a second image, called a phase image or phase contrast image. This image often provides significantly more contrast than the topographic image and has been shown to be sensitive to material surface properties, such as stiffness, viscoelasticity, and chemical composition.[19,28−30] In general, changes in phase angle during scanning are related to energy dissipation during tip−sample interaction[31] and can be due to changes in topography, tip−sample molecular interactions, deformation at the tip−sample contact, and even experimental conditions.[32−39] Because the phenomenon affecting phase image contrast is complex, an understanding of the contrast variation due to chemical and mechanical heterogeneity in polymer systems requires systematic variations of experimental variables.[19,20,29] Thus, evaluating information contained in a phase image must be done carefully and, where possible, should be done through comparison with results from other AFM methods (e.g., nanoscale indentation and lateral force or friction mode) or other analytical techniques. However, while the relationship between changes in energy dissipation and changes in material properties is not well understood, the enhanced contrast that can be obtained often allows for distinguishing different material phases and constituents.[19,30]

To directly measure changes in polymer properties on a sample surface, the atomic force microscope can be used in a nonimaging mode, called force mode, to perform nanoscale indentation studies.[40−43] In general, force mode is used to understand the tip−sample interactions.[35−39] Instead of scanning the probe laterally across the sample, the probe is positioned above a single area and moved vertically. The tip deflection, as measured with the optical lever detection system, is plotted as a function of the motion of the piezoelectric scanner in the *z* direction to produce a force curve. This force curve can be analyzed to provide information on the local elastic properties.[41−43] Using phase imaging and nanoscale indentation in combination allows the heterogeneous regions in polymer systems to be identified based on mechanical response to indentation.

The objective of the current research is to identify and characterize heterogeneity of polymers and polymer systems, so as to provide a better understanding of the mechanisms and controlling factors affecting the performance and durability of protective coatings. In this paper, research is presented to demonstrate the use of a combination of phase imaging and nanoscale indentation with the AFM to study the heterogeneity in polymer blends before and after annealing. For this purpose, blends of polystyrene (PS) and polybutadiene (PB) were chosen, because PS and PB differ significantly in thermal and mechanical properties. Nonequilibrium phase-separated structure was induced through the high solvent removal rates of the spin-coating technique used to prepare the blend samples. Thus, these samples are model materials for studying AFM phase contrast. The observed blend morphology is not important except in terms of identifying the phase-separated regions and understanding phase contrast between these regions. Further, by controlled annealing, both the chemical and mechanical properties of the PB can be changed systematically. Thus, changes in the blend samples are studied as a function of annealing to investigate the effects of surface property differences on phase image contrast and force−distance curves. Here, annealing is used only to alter the relative property differences of PB and PS regions in the blend samples, not to cause any further phase separation toward an equilibrium morphology. Results from polarity measurements, Fourier transform infrared spectroscopy (FTIR), differential scanning calorimetry (DSC), and dynamic mechanical analysis (DMA) of bulk PS and PB samples are used to assist in the interpretation of the AFM results for the PS/PB blends. The information generated can be useful in the mapping of "degradable" and "nondegradable" regions in coatings.

Materials

Polystyrene (PS) with a weight-average molecular weight, M_w, of 250 000 and polybutadiene (PB) with M_w = 420 000 were acquired from the Aldrich Company. (Certain commercial instrument and materials are identified in this paper to adequately describe the experimental procedure. In no case does such identification imply recommendation or endorsement by the National Institute of Standards and Technology and Howard University, nor does it imply that the instruments or materials are necessarily the best available for the purpose.) The PB material contained 36% cis, 55% trans, and 9% 1,2 addition (here, percentages are used to express mass fractions of material components). Blends with mass fractions of both PS and PB of 50% were prepared by mixing solutions of a mass fraction of PS of 2% in toluene and a mass fraction of PB of 2% in toluene. The PS/PB blend films were prepared by spin casting the solutions on silicon wafers at a speed of 2000 rpm for 30 s. Prior to application of the solutions, the silicon wafers were cleaned first with acetone and then methanol and dried with nitrogen. Three types of PS/PB film samples were studied: a freshly prepared blend, a conditioned blend, and an annealed blend. After spin casting, both of the conditioned samples and annealed samples were conditioned for 4 days at 24 °C ± 2 °C under vacuum before testing or thermal treatment. The annealed films were then heated in an air-vented oven at 80 °C for up to 102 h. At specified time intervals, these samples were removed from the oven for investigation using AFM. As commented previously, the blend is expected to have a nonequilibrium morphology due to the high solvent removal rates associated with spin coating. However, annealing the blend samples is not expected to alter this morphology toward an equilibrium structure but rather is used to systematically change the properties of the PB-rich regions.

In addition to the blend samples, free-standing and cast films of PB and PS were also prepared so that property changes in the PB-rich regions of the blend samples during annealing could be compared to property changes in annealed PB films. Cast PB and PS films were prepared using solutions that were 2% by mass of PB and PS, respectively, in toluene and the same spin casting procedure as that described for the blend films. Free-standing PB and PS films were made from solutions in toluene that were 10% by mass of PB and 50% by mass of PS, respectively. To form the films, a drawdown

technique was used, in which the polymer solution was flooded on a release paper, and a glass rod was firmly drawn across the paper to remove excess solution. Strips of masking tape were layered to the desired thickness and placed along the length of the release paper to control the film thickness. Both cast and free-standing PB films were annealed at 80 °C in an air-vented oven for up to 200 h. At specified time intervals, samples were removed from the oven for investigation of chemical and mechanical changes due to heating using polarity measurements, FTIR, DSC, and DMA. Both cast PS and free-standing PS films were conditioned under ambient conditions (24 ± 2 °C and 45% ± 5% relative humidity, RH) for 24 h followed by 24 h of heating at 40 °C in a vacuum oven.

Characterization Methods

TMAFM. Tapping mode AFM was performed with a Dimension 3100 (Digital Instruments) scanning probe microscope. Topographic (height) and phase images were recorded simultaneously at ambient conditions. Commercial silicon cantilever probes, each with a nominal tip radius of 5−10 nm and spring constant in the range of 20−100 N/m (values provided by manufacturer) were oscillated at their fundamental resonance frequencies, which ranged between 250 and 300 kHz. The level of tapping force used during imaging is related to the ratio of the set-point amplitude to the free-oscillation amplitude, hereafter called the set-point ratio. For example, for a set-point ratio close to but less than 1, the set-point amplitude is almost equal to the free-oscillation amplitude, and so the tip is lightly tapping on the surface. As the set-point ratio decreases from 1 toward 0, the tapping forces increase as the sample further restricts the oscillatory motion of the probe.

Depending on the operating conditions, different levels of tapping force might be required to produce accurate, reproducible images on different samples. In addition, the amount of tapping force used will often affect the phase image, particularly with regard to whether local tip−sample interactions are attractive or repulsive. For consistency with other TMAFM literature, three force levels corresponding to set-point ratios of 0.40−0.60 (hard tapping), 0.60−0.70 (moderate tapping), and 0.80−0.90 (light tapping) were investigated. All images were recorded using a free-oscillation amplitude of 145 ± 10 nm. This amplitude is relatively high compared to values used in published studies, which tend to range from 20 to 140 nm[19,20,30]. However, imaging at higher tapping amplitudes has been shown to result in more repulsive tip−sample interactions than imaging at lower amplitudes.[44] Because the primary focus of this study was to investigate changes in phase contrast based on changes in stiffness, a relatively high oscillation amplitude was chosen. In addition, the oscillation frequency was readjusted after engaging the tip on the surface such that the operating frequency was on the low-frequency side of resonance during imaging. This procedure was used to counteract any shifting of the resonance frequency to lower frequencies due to attractive tip−sample interactions, particularly those that occur during the initial approach of the tip to the sample surface.

Because silicon is a high-energy surface, it is covered with a thin layer (approximately 2.5 nm) of native SiO_2.[45] Under ambient conditions, SiO_2 readily adsorbs water, so that the outermost layer of a SiO_2 surface is covered with a high density of hydroxyl groups, approximately one silanol group per 0.6 nm^2.[46] Thus, the surfaces of the silicon tips used in this study were assumed to be covered with OH groups and thus behaved as hydrophilic materials.

AFM was also used to measure thicknesses of cast films. For this application, a section of the film was removed by toluene to expose the silicon substrate. The average step height from the film surface to the surface of the substrate was used as an estimate of the film thickness. The result reported was the average of six measurements.

To obtain mechanical responses of different domains in the blend films, nanoscale indentation was performed utilizing the same type of silicon cantilever described previously. For this application, force curves were obtained with the tip probing the regions of interest in the blend films. While more in-depth analysis of the force curves can be used to measure relative modulus values,[40,43] the identity of mechanically different regions can be inferred simply from the slope and shape of the repulsive or contact portion of the force curve. Force curves were also recorded using a sapphire sample under the same experimental conditions as those taken using the blend samples. Because the stiffness of the sapphire was very high compared to the compliant cantilever probe, the displacement of the *z*-piezo scanner after tip−sample contact resulted in displacement due to the bending of the probe; i.e., no sample penetration occurred. In general, displacement of the *z*-piezo scanner after contact can result in both probe displacement due to bending and tip penetration into the sample. Thus, force curves on sapphire served to calibrate the amount of bending displacement corresponding to a given probe deflection, so that for the same probe deflection applied to a polymer sample, the amount of tip penetration into the polymer and, hence, the relative stiffness of the polymer can be estimated.

Polarity Measurement. To estimate the change in the polarity of PB regions in the blend during annealing, contact angles of cast PB films heated for different times were measured using a Rame-Hart goniometer. Both advancing and receding angles of water and methylene iodide were recorded approximately 30 s after the drop was placed on the sample surface. A minimum of six readings was recorded for each liquid on each sample. The polar force component and the total surface free energy of PB as a function of annealing time were estimated using the geometric means approach of Owens and Wendt.[47] In this approach, the polar and nonpolar or dispersion force components of a material are calculated based on contact angle data and the polar and nonpolar components of surface tension for the two liquids. Surface tension values of 72.8 and 50.8 mJ/m^2 for water and methylene iodide,[48] respectively, and their respective polar component values of 50.7 and 1.8 mJ/m^2 were used for the calculation. For thermodynamic language consistency, we use the term surface tension for the liquids and the term surface free energy for the solids, although these terms are often used interchangeably in the literature.

FTIR Analysis. FTIR-transmission analysis of the PB films was conducted to determine the changes in PB caused by oxidation during annealing. FTIR transmission spectra of the freshly prepared and annealed PB cast samples were collected using a Nicolet 560x Fourier transform spectrometer equipped with a mercury−cadmium−telluride (MCT) detector. All spectra were acquired as 200 signal-averaged scans with a resolution of 4 cm^{-1}. The transmission spectrum of the bare silicon substrate was used as the background. The integrated intensity of carbonyl absorption in the 1650−1850 cm^{-1} region was used to determine PB oxidation in the films. Dry air was used as the purge gas.

DMA and DSC. The glass-transition temperature, T_g, of free-standing PB and PS films before annealing was recorded by DMA. In addition, the T_g and the room temperature (24 °C) storage modulus, E', of free-standing PB films after annealing for different times were measured using DSC and DMA, respectively. DSC was performed using a DSC 2910 (TA Instruments) differential scanning calorimeter equipped with a refrigerated cooling system. Samples with masses between 12 and 15 mg were sealed in an aluminum pan and subjected to a heating rate of 10 °C/min from −50 to +150 °C. DMA was carried out in a Rheometrics Solid Analyzer (RSA) II in the tensile mode at a frequency of 10 Hz and a dynamic strain of 0.0005. Films having dimensions of 12 × 35 mm^2 and thicknesses that ranged from 0.05 to 0.09 mm were used. Experiments were conducted from −140 to 150 °C, and data were recorded in 2 °C increments.

Results and Discussion

Unannealed PS/PB System. The contrast obtained in phase imaging is governed by many factors that affect tip−sample interactions, including the mechanical properties and the chemical composition of sample sur-

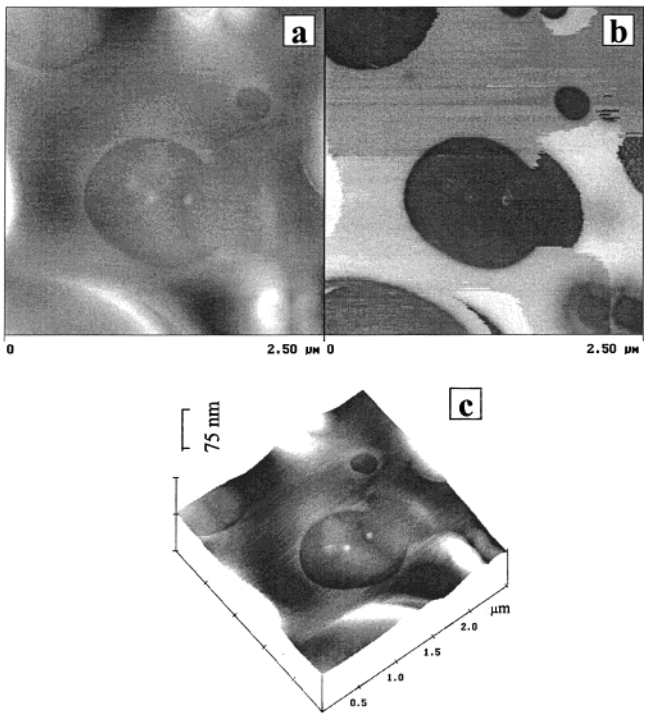

Figure 1. Tapping mode AFM (a) height image, (b) phase image, and (c) three-dimensional image of a freshly prepared 50/50 mass fraction PS/PB film on a silicon substrate. Color contrast from black to white represents a total range of 75 nm in the height image and 90° in the phase image.

faces.[19,29,30,39,49,50] To map mechanically heterogeneous domains in a polymer system using phase imaging, the contribution due to chemical effects must be minimized. Unannealed PS/PB blend films are ideal for this investigation because, mechanically, the glassy PS material is substantially different compared to the elastomeric PB material. For example, the storage modulus, E', of unannealed PB used in this study was measured using DMA to be 1.5 ± 0.1 MPa, which is almost 3 orders of magnitude lower than the value of 1.3 ± 0.1 GPa measured for unannealed PS. (Throughout this text, each number following the symbol $\pm$ is the numerical value of an estimated standard deviation.) Also using DMA, the T_g value of the freshly prepared PB film was found to be -102 ± 2 °C, while that of the freshly prepared PS film was found to be 100 ± 4 °C. However, PS and PB have similar polarities and are both essentially nonpolar materials. By use of contact angle measurements using water and methylene iodide, the polar force components of PS and PB films on silicon substrates were found to be 1.0 ± 0.2 and 0.4 ± 0.2 mJ/m^2, respectively. FTIR analysis also showed no evidence of polar C−O groups in either unannealed PB or PS films. Finally, the nonequilibrium blend morphology created by the spin-coating process provides phase-separated structure on a size scale amenable to AFM investigation. Thus, these blend samples are truly model materials for studying AFM phase contrast.

In Figure 1, a two-dimensional topographic image is shown, along with the corresponding phase image and a three-dimensional representation of the topography, for a freshly prepared PS/PB film. The magnification of this image is indicated by the scan dimension, which is 2.5 μm. The thickness of this film was 250 ± 20 nm, as measured by AFM. In this figure, topographic (height) variations of less than 20 nm are observed across the sample surface. Thus, the topography alone provides little information about the heterogeneity of the PS/PB blend film.[28] However, the phase image provides strong contrast between the different domains. The size, dispersity, shape, and spacing of the dark domains vary within the sample. Image analysis of lower magnification scans indicated that the bright and dark regions both occupied approximately 50% of the sampled area. Without further analysis, however, positive identification of the dark or bright regions in Figure 1b as being PS or PB is not possible. In general, assigning chemical composition to the features observed in height and phase images is difficult unless additional experimentation is conducted.[19] Further, the assignment of the bright or dark contrast to the hard or soft domain in phase imaging is not always straightforward. For example, several studies have assigned the brighter contrast to the stiffer material and the darker contrast to the softer material.[20,24,32,51] In other reports, the darker region has been attributed to the harder material and the lighter region to the softer material.[19,30] To provide further data for identifying the composition of the different regions, nanoscale indentation was performed.

As discussed previously, a force curve is a plot of the deflection of the free end of the AFM probe as a function of z-piezo motion as the probe approaches, contacts, and withdraws from the sample surface. This curve can be used to provide information on local properties of the sample.[40−43,52] The measured deflection of the probe is proportional to the tip−sample interaction force through the probe spring constant. To produce high force sensitivity for imaging purposes, the required spring constants are quite low (less than 100 N/m), which hinders the ability of the tip to penetrate most types of samples. For example, very little if any penetration of the probe tip into the glassy PS material occurs. However, because the elastomeric PB is extremely compliant in its unannealed state, significant penetration of the probe tip can occur. Thus, indentation measurements using these probes have the potential for distinguishing between different domains in the PS/PB blends. In addition, the hysteresis (difference between the approaching or loading curve and the retracting or unloading curve) in the force curve can be used to characterize the adhesive interaction between the tip and the sample.[35,43] The ability to use the same AFM probe for imaging and indentation combined with the ability to switch back and forth from tapping mode imaging with phase contrast to force mode indentation allows for efficient and straightforward identification of different domains.

Force curves corresponding to the darker phase domain and the brighter phase matrix from Figure 1b are shown in parts a and b of Figure 2, respectively. Several notable differences in the shape and slope of the repulsive or contact portions of the two curves are observed. The same tip deflection or applied force corresponds to a larger change in z-piezo position for the brighter matrix compared to the darker domains. During contact, changes in z-piezo position are translated into either tip deflection or penetration into the sample. Therefore, because the tip deflections were equal for the two force curves, the difference in z-piezo position corresponds to more penetration into the bright region (matrix) compared to the dark region (domain). In addition, the force curve for the bright region has a larger hysteresis and deeper trough after unloading

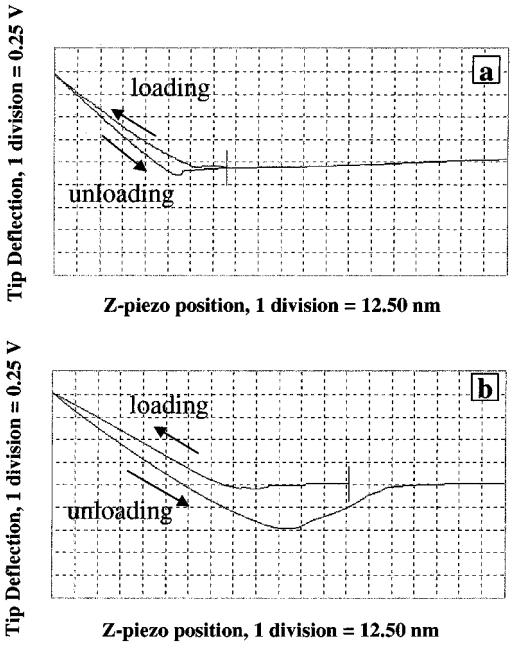

Figure 2. Typical force curve for (a) the domain and (b) the matrix in the freshly prepared 50/50 mass fraction PS/PB film.

compared to that of the dark region.[19] This behavior is characteristic of compliant materials and is caused by greater tip penetration, which creates more local inelastic deformation of the sample and higher adhesion forces due to the increased tip−sample contact area. Force curves (not shown) of individual cast PS and PB films that have comparable thicknesses to the blend samples were similar to the force curves displayed in parts a and b of Figure 2, respectively.

By use of these results, the dark domains in the phase image of Figure 1b were identified as consisting mostly of the glassy PS and the bright matrix of mostly the elastomeric PB. This assignment is consistent with other studies for different hard/soft polymeric systems, which showed that harder polymers form domains of dark contrast and softer matrices appear as bright in phase images.[19,22,53] However, it is in disagreement with that of several other reports[24,28,30,32] that attributed the darker domains to the softer materials. These contradictory assignments are not surprising because the relative contrast of different regions in phase images strongly depends on both the force level and the free-oscillation amplitude.[19] For example, Bar et al.[19] observed that both the height and phase images of hard/soft polymer blends reversed twice when changing the AFM experimental conditions. Sauer et al.[24] and McLean and Sauer[22] also reported a flipped contrast when changing from moderate to hard tapping. However, the combination of phase imaging and indentation has provided positive identification of different regions in PS/PB blends.

With this successful identification of heterogeneous polymer domains, the effect of tapping force level, indicated by the set-point ratio, on the level of phase contrast obtained using TMAFM was investigated. In parts a, b, and c of Figure 3, TMAFM height (left) and phase images (right) of a conditioned PS/PB film are shown for light, moderate, and hard tapping conditions, respectively, as defined previously. The preparation of this film was similar to that for the film imaged in Figure 1, except that this cast film has been exposed to

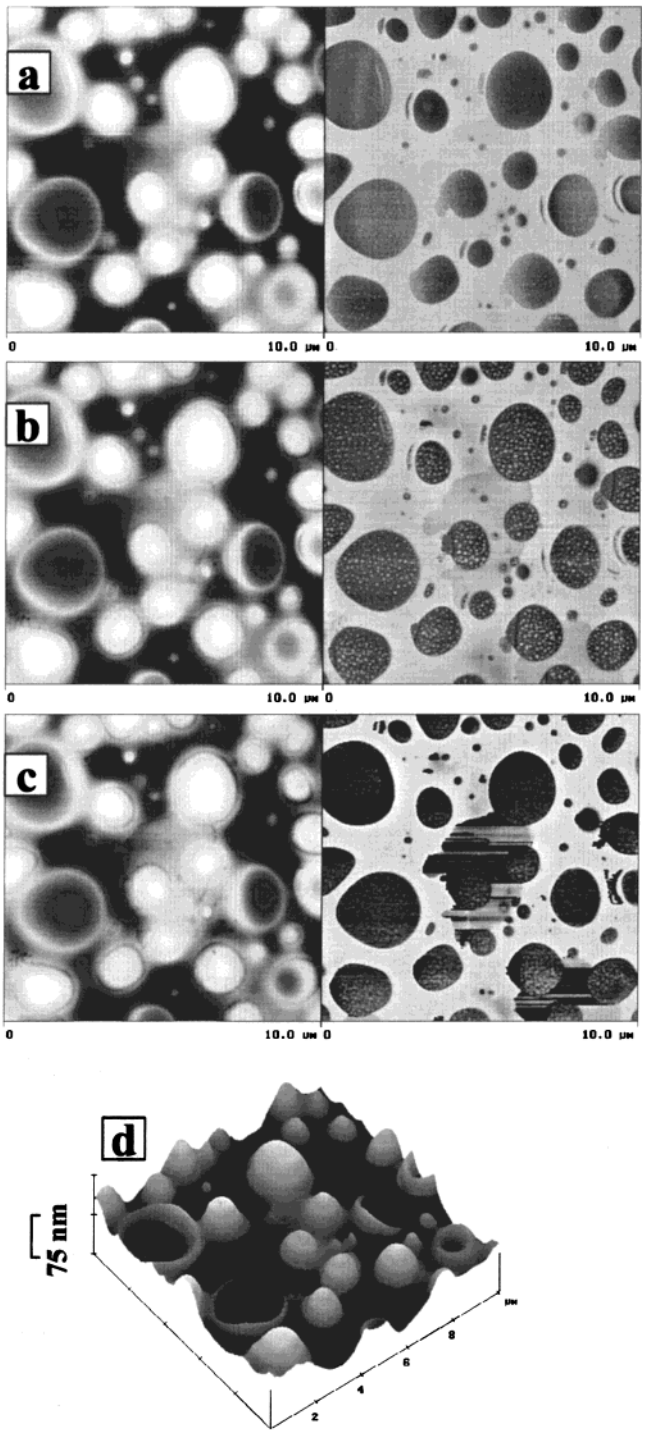

Figure 3. Tapping mode height (left) and phase images (right) of a 50/50 mass fraction PS/PB film using (a) light, (b) moderate, and (c) hard tapping. (d) Three-dimensional view of the topography shown in part b. Color contrast from black to white represents a total range of 75 nm in the height image and 90 ° in the phase image.

ambient conditions (24 ± 2 °C and 45% ± 5% RH) for 4 days. Again, the thickness of this film was approximately 250 ± 25 nm, as measured by AFM. To better understand the height variation between PB and PS in the blend, a three-dimensional image of the topographic data in Figure 3b is shown in Figure 3d. The change in the contrast between the dark and bright areas in the height images (left) is minimal when the force level is increased from light to hard tapping. However, the contrast of the phase images (right) is greatly enhanced

with an increase in the force level. The glassy PS domains become much darker and the PB matrix turns slightly brighter at hard tapping. This change in phase contrast was both reversible and repeatable during subsequent decreases and increases in tapping force level.

One notable observation of the phase image results for this PS/PB film is that no contrast reversal occurs when the force is varied from light to moderate to hard tapping. Bar et al.,[19] McLean et al.,[22] Sauer et al.,[24] and Magonov et al.[30] reported contrast flipping when changing the tapping force level for some hard/soft polymer systems. Such contrast flips generally occur due to changes in the tip−sample interaction between attractive and repulsive force regimes, which can occur on different regions of the sample at different tapping force levels.[54] In the present study, the readjustment of the oscillation frequency to the low-frequency side of resonance after tip−sample contact might have prevented such contrast flipping. Most likely, tip−sample interactions were repulsive for both phase-separated regions under the imaging conditions (e.g., high oscillation amplitude)[44] used in this study, resulting in a systematic change in contrast as a function of tapping force level.[55] However, artifacts are observed in the phase images of Figures 1 and 3 that appear as streaks or alterations of the phase contrast for the matrix regions near the edges of some of the domains. These artifacts might be caused by changes in the tip−sample interaction that are related to shifts of the resonance frequency with respect to the operating frequency. Such frequency shifts should also alter the oscillation amplitude and cause related artifacts in the topographic images. For example, topographic artifacts are observed in Figure 1a that correspond to the phase artifacts in Figure 1b. The streaking artifact in Figure 3c, however, does not have any associated topographic artifacts. In fact, the topographic image in Figure 3c appears to be very similar to that in Figure 3b where no streaks are observed in the phase image.

The enhanced contrast of the PS domain at hard tapping in Figure 3 suggests that, as the force level increases, the phase changes of the oscillating cantilever are largely governed by the local sample stiffness. In addition, the phase contrast for the areas in the middle and lower right of the phase images in Figure 3, i.e., where the streaking artifacts occur in Figure 3c, seems to increase with an increase in the tapping force level. Note that the height level of these areas is between that of the PS domains and the PB matrix. Perhaps in these areas, a thin layer of the PB material resides above several PS domains.[56] At high tapping forces, these areas become darker in the phase image, because the stiffness of the PS present underneath the thin layer of PB becomes more important and reduces the phase shift. Further, in Figure 3c, the streaking artifact that occurs in the phase image could be caused by slight changes in the thickness of the PB layer or local changes in the relative contribution of the underlying PS domains to the phase response of the AFM probe during hard tapping. No corresponding topographic artifacts would be expected, as is the case.

Phase imaging also allows the observation of the size distribution of the glassy PS domains in the elastomeric PB matrix. Larger oval-shaped domains of up to 2.7 μm in size coexist with smaller domains that are 50−100 nm in size. Further examination of the phase images in Figure 3b reveals a microphase separation within the PS domains. Both large and small PS domains contain small "droplets" with a bright phase level that is similar to that of the PB matrix. High-resolution phase imaging (not shown) revealed that the droplets are nonspherical and have sizes ranging from 10 to 50 nm. Further, the phase contrast between the droplets and the enclosed domains is greatest under moderate tapping conditions (Figure 3b). Under hard tapping conditions (Figure 3c), the phase contrast between the droplet and the domain becomes poor and the droplets are barely visible. Under careful examination, these small particles can also be observed in some portions of the topographic images in Figure 3 (left). The droplet regions are believed to be made up of PB molecules trapped within the glassy PS domains. The presence of the matrix phase as tiny droplets within the domains during the late stages of phase separation has been previously observed for PS/PB and other blends.[20,57,58] The process is commonly related to hydrodynamic instability of the matrix, leading to "double phase separation". However, as discussed previously, this morphology occurs in the present study under processing conditions that result in nonequilibrium structures.

Unlike the freshly prepared sample of Figure 1, a distinct morphological pattern is evident in the height images for the conditioned sample shown in Figure 3. Except for a few locations, the bright areas and dark areas in the height images (see Figure 3) generally correspond to the dark domains and bright matrix in the phase images, respectively. The glassy PS domains are often the bright areas (higher topography) and the elastomeric PB corresponding to lower topography. In Figure 3d, the few PS domains that are mostly dark in the height images appear to be "hills" that have collapsed into valleys. In the phase images, the collapsed areas still appear as dark domains, indicating that they consist mostly of PS material. Further, because the phase contrast of these collapsed hills is constant throughout each domain region, despite the topographic variations, and is the same for collapsed and intact hills, the unusual topographic structure of these features is believed to be real. If the topographic structure of the PS domains was not real, changes in topography might be expected with changes in imaging conditions. In addition, the same type of topographic structure might not be observed upon reimaging, particularly after alteration of the sample. However, as observed in Figures 3 and 4, the topography of the numerous PS domains in one particular area remains constant with increasing tapping force (see Figure 3), and similar topographic features are observed in different areas of the sample after various annealing times (see Figure 4). Thus, the results of phase imaging can help to verify features in a polymeric mixture that may have caused confusion interpreted solely on the basis of topographic information. On the basis of these results, the glassy PS material appears to form hills and the elastomeric PB occupies lower regions for the conditioned PS/PB blend film sample. Further, the height variation for the freshly prepared sample is approximately 20 nm, whereas that of the conditioned sample is approximately 60 nm. This difference is probably due to the latter reaching a later stage of phase separation compared to the former, although in both cases a nonequilibrium structure has resulted.

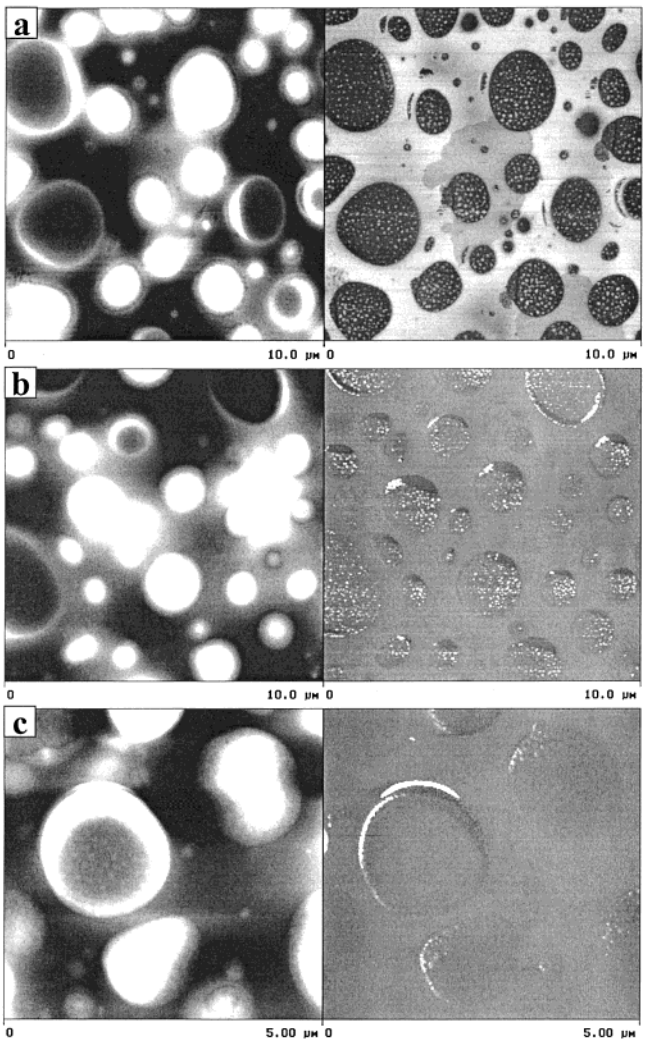

Figure 4. Height (left) and phase images (right) using moderate tapping forces for a 50/50 mass fraction PS/PB film that had been annealed at 80 °C in air for (a) 0, (b) 60, and (c) 102 h. Color contrast from black to white represents a total range of 75 nm in the height image and 90° in the phase image.

Annealed PS/PB Systems. To map domains having different chemical properties using phase imaging, the effects of the chemical and mechanical contributions on the phase signal must be maximized and minimized, respectively. Although PB is essentially a hydrophobic polymer, it is susceptible to thermal oxidation.[59,60] When heated in air, various oxygenated groups are formed in PB and cross-linking occurs that, as will be shown, causes an increase in its T_g and modulus. By adjusting the state of oxidation and thus cross-linking of the film, the polarity and the mechanical properties of PB can be varied so that their effects on the phase contrast of the PS/PB system can be systematically changed.

In Figure 4, the height (left) and phase (right) images of a PS/PB blend film that had been annealed at 80 °C in air for several time intervals using moderate tapping are presented. The images shown in Figure 4a are the same as those in Figure 3b for comparison of annealed samples with an unannealed sample. The images in Figure 4c are at a higher magnification, but that does not hinder comparison between the three sets of images. Very little change in topography is observed in the height images upon annealing. The PS material continues to occupy the high domains and PB matrix occupies the valleys, and the average height variation between the two regions in the heated samples is similar to that of the conditioned but unannealed samples, approximately 60 nm. However, the contrast of the phase images greatly changes as a result of heating. Except at some edge areas, the contrast between the PS domains and the PB matrix is substantially reduced after 60 h and becomes negligible after 102 h of heating. Further, after 60 h of heating, the small droplets of PB trapped in the PS domains still maintain a bright contrast. At long heating times (see Figure 4c), the contrast difference between most of the droplets and the PS domains disappears.

These results may provide qualitative insight concerning the relative contribution of the mechanical and chemical properties on the phase contrast for the PS/PB system. With increasing heating time in air, both the polarity and the modulus of the PB component in the blend are expected to increase while these properties for the more thermally stable PS should remain mostly unchanged.[61] As the stiffness of PB approaches that of PS and the polarity of the former is greater than that of the latter, the mechanical contribution to the contrast should diminish and the chemical contribution should be enhanced. However, little visible contrast difference between the PS domains and the PB surrounding or between the PS domain and the PB droplets is observed for samples annealed for a long time in air, as shown in Figure 4c. These results indicate that, under the conditions used in this experiment, i.e., moderate tapping at a relatively high free-oscillation amplitude of 145 ± 10 nm, the phase contrast observed in Figure 4 is mostly due to differences in the mechanical properties of the two components. The effect of differences in chemical properties is not detected in these images. This observation is consistent with the study by Brandsch et al.[44] in which higher tapping amplitudes resulted in repulsive tip−sample interactions such that the phase contrast was dominated by sample stiffness.

After 60 h of heating, the PB droplets have much brighter phase contrast with respect to the PS domains compared to the minimal contrast of the PB matrix (see Figure 4b). This observation might be related to a difference in stiffness between the PB molecules trapped in the glassy PS domains and the PB matrix. This difference in stiffness is probably due to the hindered diffusion of oxygen through the glassy PS layer to the trapped PB molecules such that no cross-linking occurs. On the other hand, the oxygen-accessible PB molecules in the blend matrix are fully oxidized and significant cross-linking has occurred after the same period of heating. After being annealed further (Figure 4c), only a few bright droplets can be distinguished in the PS domains, probably because for most of them oxidization and cross-linking has occurred, producing for the droplets stiffnesses similar to those of the PS domains and PB matrix.

To verify that the PB matrix in the blends was increasingly oxidized and stiffened during annealing, the carbonyl formation and growth, the polarity, the storage modulus (E'), and the glass-transition temperature (T_g) of PB films were measured as a function of annealing time, with annealing performed in air at 80 °C. Carbonyl formation and polarity were determined on PB films cast on silicon substrates using FTIR-transmission spectroscopy and contact angle measurements, respectively. The FTIR-transmission spectroscopy measures C═O groups for the entire 250 nm film

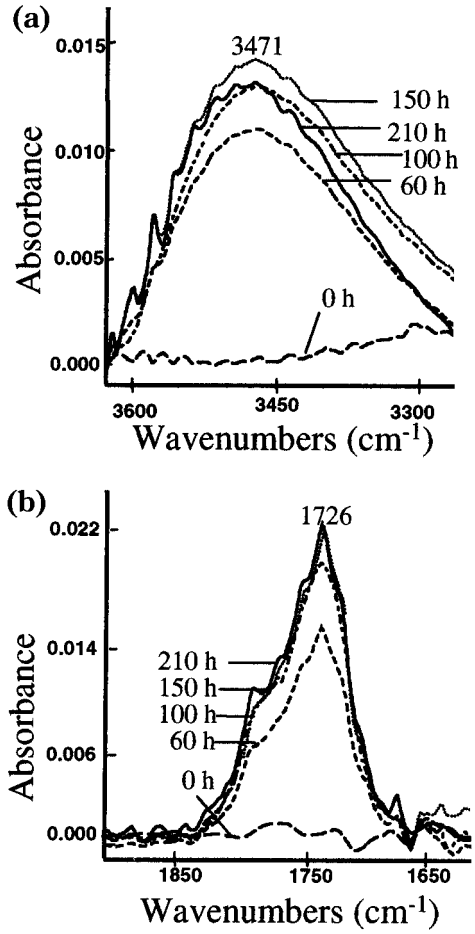

Figure 5. FTIR-transmission spectra in the (a) 3620−3250 and (b) 1900−1600 cm^{-1} regions showing the effects of heating at 80 °C in air for a cast PB film.

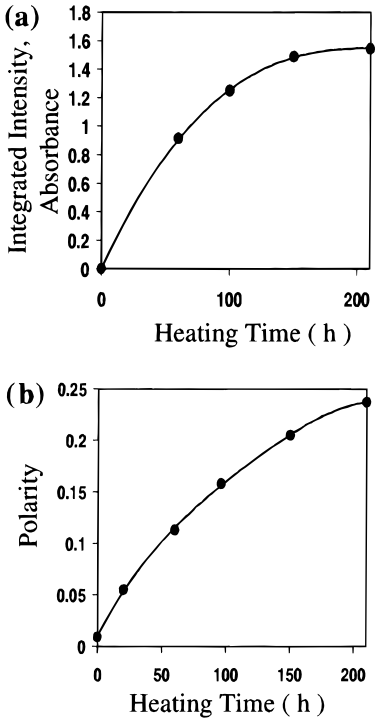

Figure 6. (a) Carbonyl intensity and (b) polarity of a cast PB film as a function of heating time at 80 °C in air.

thickness. Thus, FTIR intensity represents the total concentration of these groups in the bulk film. On the other hand, polarity was calculated based on contact angle measurements, and therefore, it represents the total polar component of the surface. In addition, other oxygenated products besides the C=O groups are formed during annealing. Thus, FTIR intensity for the C=O groups only provides the state of oxidation and does not represent the polarity of the film. The thickness of the PB films used for these measurements was 500 ± 25 nm, which was approximately twice that of the PS/PB blend film thicknesses. The free-standing films of PB used for measuring the T_g and E' were even thicker, with thicknesses of 75 ± 10 μm. Because the PS/PB blend films were thinner than both the cast and free-standing films of PB, the PB portion of the blend is assumed to have attained similar chemical and mechanical properties at heating times shorter than those for the PB films. The AFM results shown in Figure 4, which show little contrast difference between the PS domain and the PB matrix after 60 h of annealing, support this assumption.

The FTIR-transmission spectra for wavenumbers of 1600−1900 and 3250−3625 cm^{-1} for a cast PB film on a silicon substrate are displayed in Figure 5 for several heating times. Extensive oxidation occurs in the film, as indicated by the appearance, followed by an increase in the intensity, of the C=O bands in the range of 1700−1750 cm^{-1} and the OH bands in the range of 3050−3650 cm^{-1}. The C=O intensity increases rapidly in the first 100 h and then slows thereafter, as shown in Figure 6a. Similarly, the polar component of the surface free energy increases with heating time from 0.4 ± 0.2 mJ/m^2 for a freshly prepared sample to 10.8 ± 0.2 mJ/m^2 after 200 h. This increase translates to an increase in polarity from 0.009 to approximately 0.24, as shown in Figure 6b. For comparison, the polarity values of poly(hexamethylene adipate), one of the more polar polymers, and poly(methyl methacrylate) are 0.21 and 0.10, respectively, using the same polarity estimation method.[62] The rate difference between the C=O intensity curve and the polarity curve at long heating times is probably related to the formation of oxygenated products from reactions of some C=O groups or the formation of other polar groups, such as OH, as seen in Figure 5a.

Annealing of PB in air also caused a decrease in the advancing contact angle of water from 93° ± 3° for a freshly prepared sample to 66° ± 4° after 200 h of heating. However, no corresponding change in the advancing contact angle of methylene iodide, which was 36° ± 2°, was observed. The contact angle hysteresis (advancing angle minus receding angle) of water also increased, from 18° ± 4° before heating to approximately 30° ± 2° after 200 h of heating, reflecting an increase in the heterogeneity of the annealed PB surface. In addition, the total surface free energy (polar component + nonpolar component) of the PB surface was found to increase from 41.7 to 46.0 mJ/m^2, after 200 h of heating in air. Thus, the annealed PB surface was more energetic than the unannealed material. Because surface free energy is a function of surface chemical composition, any change in the surface free energy, particularly the polar component and the total surface energy, would affect the tip−sample interactions.

The effect of any of the surface free energy parameters on the phase contrast of Figure 4 is unknown. Noy et al.[39] recently reported a direct correlation between tip−sample adhesion obtained in solvents and phase lag. In

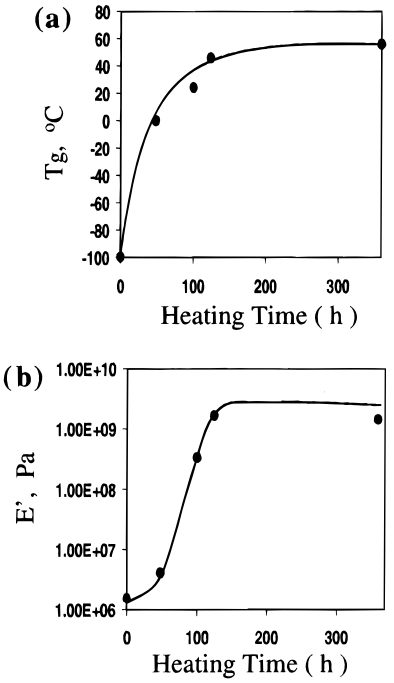

Figure 7. (a) T_g and (b) E' of a free-standing PB film for several heating times at 80 °C in air.

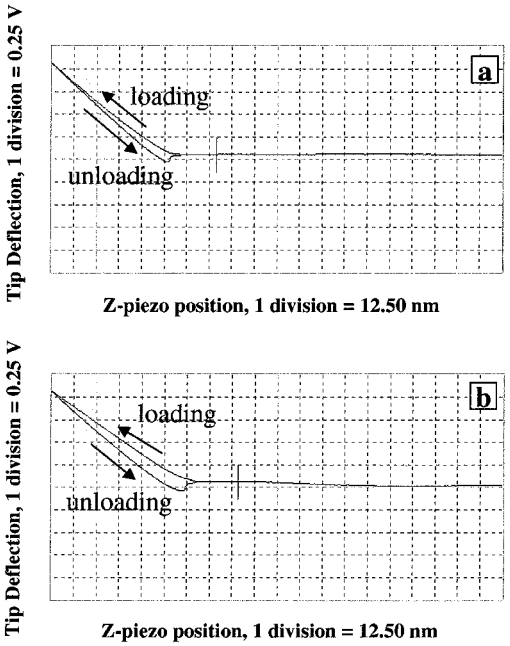

Figure 8. Typical force curves for (a) the PS domain and (b) the PB matrix for a PS/PB film heated for 102 h.

other words, increasing the adhesion forces between the tip and the sample leads to an increase in the phase lag of the oscillating probe. However, this study was conducted in a liquid environment, and the role of the solvent in the tip−sample interactions is rather complex and not completely understood.[63] In air, large attractive capillary forces are present between hydrophilic tips and hydrophilic samples[38,64−66] that affect the tip−sample interactions. However, the tip−sample interactions measured in a water medium relate to the work required to exclude the water from the tip−sample interface.[38] Thus, the interactions occurring in a water medium are repulsive interactions, consisting of electrostatic repulsion between charged surfaces, electric double-layer repulsion, and hydration shell interactions.[67] Therefore, factors affecting phase contrast for ambient conditions are not likely to be related to the factors affecting phase contrast for liquid environments.

The effects of annealing on T_g and E' of a free-standing PB film are presented in Figure 7. Despite the fact that the film was relatively thick, its T_g rose rapidly within the first 125 h of heating and then leveled off, reaching 56 °C after 360 h of annealing. Except for the first 50 h, the change with heating time of the storage modulus was similar to that of T_g, increasing rapidly and then leveling off at approximately 1.55 GPa. This value is 3 orders of magnitude greater than that of the PB samples before heating. After the same period of annealing, no change in either T_g (104 °C) or E' (1.3 GPa) of the pure PS film was observed. Although the T_g value of the annealed PB film was still lower than that for the PS bulk film (56 °C compared to 104 °C), it was still higher than ambient temperature, and E' for annealed PB was slightly higher than that for annealed PS. If similar behavior is assumed for the PB regions in the annealed PS/PB blend, both the PS and PB regions in the blends should behave as glassy materials during AFM analysis. To verify this assumption, force curves were measured for the two regions after 102 h of heating, the results of which are illustrated in Figure 8. In contrast to the force curves for the unheated samples (see Figure 2), only a small difference exists between these two curves, both of which are similar to that of the pure PS material. Thus, the mechanical property results for the pure PS and PB films correlate well with the nanoscale indentation results on the PS and PB regions of the blend.

Fully Annealed PS/PB System. As demonstrated, after prolonged heating in air, the polarity of the PB regions in a PS/PB system increased substantially while that of the PS remained unchanged. Further, by controlling the annealing time, the stiffness difference between the PS domain and the PB matrix was minimized. Thus, the phase contrast of a fully annealed PS/PB system can be attributed to differences in chemical composition. Results from the investigation of the effect of force level on phase contrast for the annealed PS/PB sample are shown in Figure 9. In parts a, b, and c of Figure 9, TMAFM images are presented for a 102 h heated PS/PB blend film using light, moderate, and hard tapping, respectively. Figure 9d is a three-dimensional representation of the topography of this sample, showing the hills of PS material and valleys of PB matrix. These images are for the same sample as that of Figure 4 for the long heating time. As indicated previously, the PB matrix in this film has been substantially oxidized, and its surface polarity has increased substantially. In Figure 9a, a visible contrast difference between the PS domains and the PB matrix under light tapping conditions is observed; i.e., the less polar PS domains have a slightly darker color than the more polar PB matrix after annealing. This result is noteworthy and will be discussed later. In Figure 9b,c, almost no contrast difference is observed between the two regions under moderate and hard tapping conditions. However, at hard tapping, a visible contrast difference between the small droplets and the PS domain is observed. This result suggests that the trapped PB molecules in the glassy PS material were probably not as fully oxidized or cross-linked as the PB molecules in the blend matrix after 102 h of heating, as discussed previously.

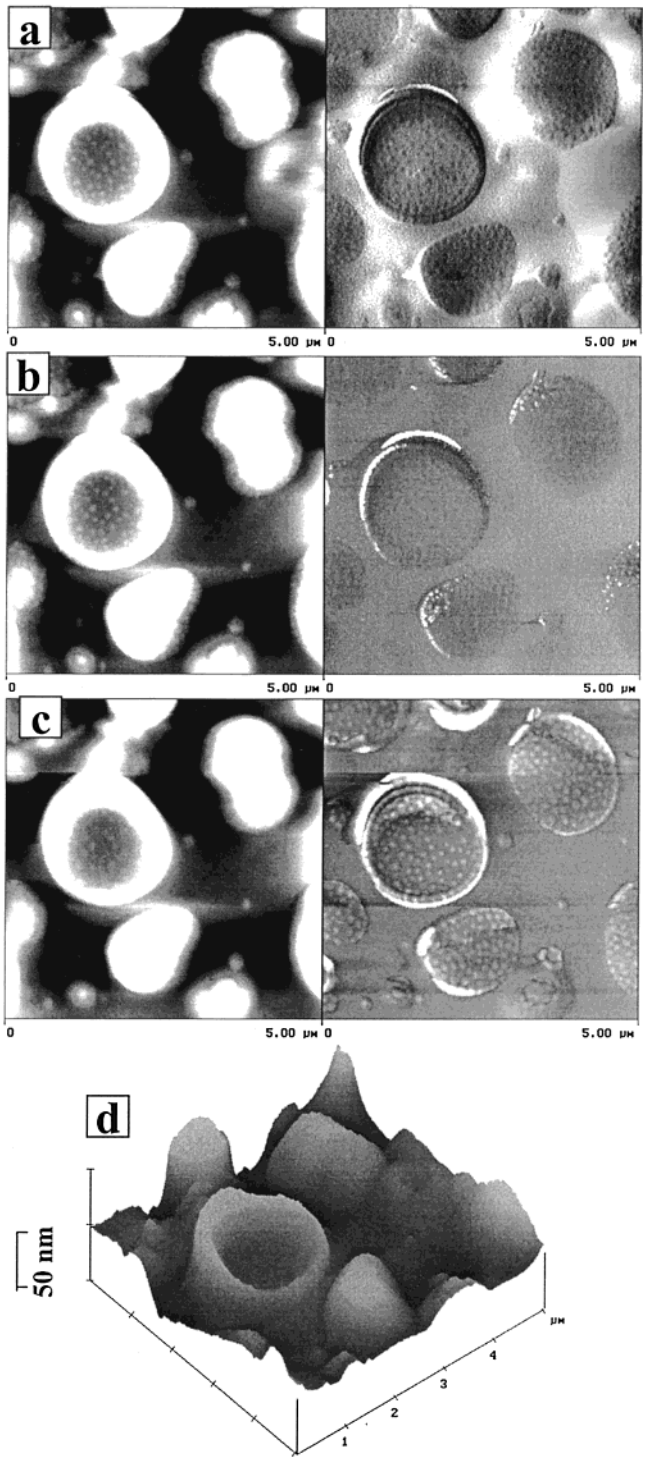

Figure 9. Tapping mode height (left) and phase images (right) for a PS/PB film after 102 h of heating. Images made using (a) light, (b) moderate, and (c) hard tapping conditions. (d) Three-dimensional view of the topography shown in part b. Color contrast from black to white represents a total range of 75 nm in the height image and 90° in the phase image.

The results presented in Figures 4b and 9c suggest that phase imaging might be useful for monitoring the curing of polymer systems.[51] As shown in these figures and from observations of other studies,[19,20,30] phase image contrast is sensitive to local film stiffness under proper experimental conditions. In addition, the mechanical properties of a polymer are a function of the extent of cure. Contrast is easily quantified using computer image analysis, and degree of cure is conveniently measured by a number of physical or chemical methods. Thus, the relationship between phase image contrast and degree of cure could be easily investigated. If such a relationship is found, AFM phase imaging may have the potential to characterize the degree of cure in the polymer bulk and in polymer/substrate and polymer/filler interphases.[51] The latter application is particularly appealing because it might provide the information needed to understand the performance and durability of important polymer systems, such as coatings, adhesives, and polymer composites.

The darker phase contrast of the less polar PS domains compared to that of the more polar PB matrix of Figure 9a is consistent with recent AFM results for PS/PMMA blends (not shown). In phase images of this system, the more polar PMMA domains appear brighter than the less polar PS regions. Because PMMA and PS have similar values of modulus and T_g,[68] the contrast differences between the PMMA and PS regions are due to factors other than local stiffness. The reason for the darker contrast in the less polar PS regions in both PS/annealed PB and PS/PMMA blend films is not clear at this time. As discussed previously, the contrast mechanisms in phase imaging are very complex and are not well understood. Besides surface mechanical properties,[19,29,30,49,69] many other factors can be responsible for phase contrast, including surface topography,[49,70] interactions between tips and samples with different chemical functionalities,[36,39,64] and capillary forces due to a water layer on the tip or sample surface.[49,65,66,69,70] In addition, instrumental and environmental conditions used during imaging also can affect the contrast obtained by phase imaging.[19,30,44] Work is being carried out in our laboratories using chemically functionalized tips and samples under different instrumental and environmental conditions to better understand the contrast difference between less and more polar domains in polymer films and highly heterogeneous regions in coating systems.

Conclusions

The following conclusions can be drawn from phase imaging and nanoscale indentation studies of PS/PB thin films using the atomic force microscope:

1. Spin-coated PS/PB blend films are useful model materials for evaluating phase contrast in tapping mode atomic force microscopy (TMAFM) because of the nanoscale and microscale phase-separated, nonequilibrium structures that have very different surface properties. In addition, annealing of the blend samples allows the relative differences in the surface properties of the phase-separated regions to be controlled systematically.

2. The level of tapping force applied to the tip was found to substantially influence the phase image contrast of the PS/PB blends.

3. Indentation with the atomic force microscope can be used effectively to distinguish the elastomeric phase from the glassy phase in a PS/PB blend. The combination of nanoscale indentation and phase imaging was used to identify PS as the material associated with higher topography regions and PB as the material associated with the lower lying regions in the height image. In addition, phase imaging at proper force levels revealed a microphase of PB droplets within the PS domains.

4. As the blend was annealed, the PB stiffness increased and the phase image contrast between PS and

PB areas decreased, indicating that mechanical properties were mainly responsible for the phase contrast between elastomeric PB and glassy PS under the scanning conditions used.

5. Under light tapping, a slight contrast difference exists between the less polar PS domain and the more polar PB matrix after 102 h of annealing. The factors contributing to this contrast difference are unknown.

6. Although phase imaging, when used with nanoscale indentation, is a powerful technique for studying mechanically heterogeneous regions, its capability for detecting chemically heterogeneity in polymer films requires further investigation.

7. Phase imaging may provide a useful tool for monitoring the degree of cure in polymer films and polymer/substrate and polymer/filler interphases.

Acknowledgment. This work was supported by the Air Force Office of Scientific Research under Grant # F49620-98-1-0252.

References and Notes

(1) Reynolds, L. B.; Twite, R.; Khobaib, M.; Donley, M. S.; Bierwagen, G. P. *Prog. Org. Coat.* **1997**, *32*, 31.
(2) Nguyen, T.; Hubbard, J. B.; Pommersheim, J. M. *J. Coat. Technol.* **1996**, *68*, 45.
(3) Raghavan, D.; Egwim, K. C. *J. Appl. Polym. Sci.*, in print, 2000.
(4) Bascom, W. D. *J. Adhes.* **1970**, *2*, 168.
(5) Mayne, J. E. O.; Mills, D. J. *J. Oil Color Chemists Assoc.* **1975**, *58*, 155.
(6) Corti, H.; Fernandez-Prini, R.; Gomez, D. *Prog. Org. Coat.* **1982**, *10*, 5.
(7) Mills, D. J.; Mayne, J. E. O. In *Corrosion Control by Organic Coatings*; Leidheiser, H., Ed.; National Association of Corrosion Engineers: Houston, TX, 1981; p 12.
(8) Wu, C. L.; Zhou, X. J.; Tan, Y. J. *Prog. Org. Coat.* **1995**, *25*, 379.
(9) Miskovic-Stankovic, V. B.; Drazic, D. M.; Teodorovic, M. J. *Corrosion Sci.* **1995**, *37*, 241.
(10) Kinsella, E. M.; Mayne, J. E. O. *Br. Polym. J.* **1969**, *1*, 173.
(11) Mayne, J. E. O.; Scantleburg, S. *Br. Polym. J.* **1970**, *2*, 240.
(12) Fernandez-Prini, R.; Corti, H. *J. Coat. Technol.* **1977**, *49*, 62.
(13) Dunn, R. C.; Hotom, G. R.; Mets, L.; Xie, X. S. *J. Phys. Chem.* **1994**, *98*, 3094.
(14) Karim, A.; Satija, S. K.; Han, C. C.; Slawecki, T. M.; Kumar, S. K.; Russell, T. P. *Polym. Prepr. (Am. Chem Soc., Div. Polym. Chem.)* **1994**, *71*, 280.
(15) Sung, L.; Douglas, J. F.; Han, C. C. *Phys. Rev. Lett.* **1996**, *76*, 4368.
(16) McEvoy, R.; Krause, S.; Wu, P. *Polymer* **1998**, *39*, 5223.
(17) Hasegawa, H.; Hashimoto, T. *Polymer* **1992**, *33*, 475.
(18) Winograd, N. *Anal. Chem.* **1993**, *65*, 622A.
(19) Bar, G.; Thomann, Y.; Brandsch, R.; Cantow, H. J.; Whangho, M. H. *Langmuir* **1997**, *13*, 3807.
(20) Bar, G.; Thomann, Y.; Brandsch, R.; Whangho, M. H. *Langmuir* **1998**, *14*, 1219.
(21) Zhang, D.; Gracias, D. H.; Ward, R.; Gauckler, M.; Tian, Y.; Shen, Y. R.; Somarjai, G. A. *J. Phy. Chem. B.* **1998**, *102*, 6225.
(22) McLean, R. S.; Sauer, B. B. *Macromolecules* **1997**, *30*, 8314.
(23) Akhremitchev, B. B.; Mohney, B. K.; Marra, K. G.; Chapman, T. M.; Walker, G. C. *Langmuir* **1998**, *14*, 3976.
(24) Sauer, B. B.; McLean, R. S.; Thomas, R. R. *Langmuir* **1998**, *14*, 3045.
(25) Bierwagen, G. P.; Twite, R.; Chen, G.; Tallman, D. E. *Prog. Org. Coat.* **1997**, *32*, 25.
(26) Shao, Z.; Yang, J. Q. *Rev. Biophys.* **1995**, *28*, 195.
(27) Umemura, K.; Arakawa, H.; Ikai, A. *Jpn. J. Appl. Phys. Part 1* **1993**, *2*, L1711.
(28) Vishwanathan, R.; Tian, J.; Marr, D. W. M. *Langmuir* **1997**, *13*, 1840.
(29) Tamayo, J.; Garcia, R. *Langmuir* **1996**, *12*, 4430.
(30) Magonov, S. N.; Ellings, V.; Whangbo, M. H. *Surf. Sci.* **1997**, *375*, L385.
(31) Cleveland, J. P.; Anczykowski, B.; Schmid, A. E.; Elings, V. B. *Appl. Phys. Lett.* **1998**, *72*, 2613.
(32) Magonov, S. N.; Elings, V.; Papkov, V. S. *Polymer* **1997**, *38*, 297.
(33) Anczykowski, B.; Kruger, D.; Fuchs, H. *Phy. Rev. B.* **1996**, *53*, 15485.
(34) Winkler, R. G.; Spatz, J. P.; Sheiko, S.; Moller, M.; Reinker, P.; Marti, O. *Phy. Rev. B* **1996**, *54*, 8908.
(35) Frisbe, C. D.; Rozsnyai, L. F.; Noy, A.; Wrighton, M. S.; Leiber, C. M. *Science* **1994**, *265*, 2071.
(36) Finot, M. O.; McDermott, M. T. *J. Am. Chem. Soc.* **1997**, *119*, 8564.
(37) Green, D. J.-B.; McDermott, M. T.; Porter, M. D. *J. Phys. Chem.* **1995**, *99*, 10960.
(38) Siinniah, S. K.; Steel, A. B.; Miller, C. J.; Reutt-Robey, J. E. *J. Am. Chem. Soc.* **1996**, *118*, 8925.
(39) Noy, A.; Sanders, C. H.; Vezenov, D. V.; Wong, S. S.; Leiber, C. M. *Langmuir* **1998**, *14*, 1508.
(40) VanLandingham, M. R.; Dagastine, R. R.; Eduljee, R. F.; McCullough, R. L.; Gillespie, J. W., Jr. *Composites A* **1999**, *30*, 75.
(41) Howard, A. J.; Rye, R. R.; Houston, J. E. *J. Appl. Phys.* **1996**, *79*, 1885.
(42) Hues, S. M.; Draper, C. F.; Colton, R. J. *J. Vac. Sci. Technol.* **1994**, *12*, 2211.
(43) VanLandingham, M. R.; McKnight, S. H.; Palmese, G. R.; Eduljee, R. F.; Gillespie, J. W., Jr., McCullough, R. L. *J. Mater. Sci. Lett.* **1997**, *16*, 117.
(44) Brandsh, R.; Bar, G.; Whangbo, M. H. *Langmuir* **1997**, *13*, 6349.
(45) Nguyen, T.; Byrd, W. E.; Bentz, D. *J. Adhes.* **1995**, *48*, 169.
(46) Zettlemoyer, A. C. *Chemistry and Physics of Interface*; Gufhee, D. E., Ed.; Am. Chem. Soc.: Washington, D.C., 1965; Chapter 12.
(47) Owens, D. K.; Wendt, R. C. *J. Appl. Polym. Sci.* **1969**, *13*, 1741.
(48) Wu, S. *Polymer Interface and Adhesion*; Marcel Dekker: New York, 1982; p 151.
(49) Schmitz, I.; Schreiner, M.; Friedbacher, G.; Grasserbauer, M. *Appl. Surf. Sci.* **1997**, *115*, 190.
(50) Vezenov, D. V.; Noy, A.; Rozsnyai, L. F.; Lieber, C. M. *J. Am. Chem. Soc.* **1997**, *119*, 2006.
(51) VanLandingham, M. R.; Eduljee, R. F.; Gillespie, J. W. *J. Appl. Polym. Sci.* **1999**, *71*, 699.
(52) Burnham, N. A.; Kulik, A. J.; Gremaud, G. In *Procedures in Scanning Probe Microscopy*; Cotton, R. J., Ed.; John Wiley: New York, in press.
(53) Leclere, P.; Lazzaroni, R.; Bredas, J. L.; Yu, J. M.; Dubois, P.; Jerome, R. *Langmuir* **1996**, *12*, 4317.
(54) Haugstad, G.; Jones, R. R. *Ultramicroscopy* **1999**, *76*, 77.
(55) Whangbo, M. H.; Bar, G.; Brandsch, R. *Surf. Sci.* **1998**, *411*, L794.
(56) Karim, A.; Slawecki, T. M.; Kumar, S.-K.; Douglas, J. F.; Satija, S. K.; Han, C. C.; Russell, T. P.; Liu, Y.; Overney, R.; Sokolov, J.; Rafallovich, M. H. *Macromolecules* **1998**, *31*, 857.
(57) Siggin, E. D. *Phys. Rev. A.* **1979**, *20*, 595.
(58) McMaster, L. P. *Adv. Chem. Ser.* **1975**, *142*, 43.
(59) Dikkie, R.; Carter, R. O., III; Hammond, J.; Parsons, J.; Holubka, J. W. *Ind. Eng. Chem. Prod. Res. Dev.* **1984**, *23*, 297.
(60) Beavan, F. W.; Philips, D. *Rubber Chem. Technol.* **1975**, *48*, 692.
(61) Israeli, V.; Lacoste, J.; Lemaire, J.; Singh, R. P.; Sivaram, S. *J. Polym. Sci. Polym. Chem.* **1994**, *32*, 485.
(62) Wu, S. *Polymer Interface and Adhesion*; Marcel Dekker: New York, 1982; p 180.
(63) Van Der Vegte, E. W.; Hadziioannou, G. *J. Phys. Chem., B.* **1997**, *101*, 9563.
(64) Vezenov, D. V.; Noy, A.; Rozsnyai, L. F.; Lieber, C. M. *J. Am. Chem. Soc.* **1997**, *119*, 2006.
(65) Eastman, T.; Zhu, D.-M. *Langmuir* **1996**, *12*, 2859.
(66) Binggeli, M.; Mate, C. M. *Appl. Phys. Lett.* **1994**, *65*, 415.
(67) Han, T.; Wialliams, J. W.; Beeke, T. P., Jr. *Anal. Chim. Acta* **1995**, *307*, 365.
(68) Nielsen, L. E. *Mechanical Properties of Polymers*; Reinhold Publishing Corporation: New York, 1967.
(69) Spatz, J. P.; Sheiko, S.; Moller, M.; Winkler, R. G.; Reineker, P.; Marti, O. *Nanotechnology* **1995**, *6*, 40.
(70) Chen, X.; McGurk, S. L.; Davies, M. C.; Roberts, C. J.; Shakesheff, K. M.; Tendler, S. J. B.; Williams, P. M.; Davies, J.; Dawkes, A. C.; Domb, A. *Macromolecules* **1998**, *31*, 2278.

MA991206R